Building Serv. Eng. Res. Technol. **11**(1) 21–26 (1990) Printed in Great Britain

Summary We describe the use of the constant injection tracer gas technique to study turbulent flow in a rectangular duct. A comparison between tracer gas measurements and measurements made using a hot-wire anemometer and a pitot tube is presented. Tracer gas concentration, air velocity and pressure distribution were measured at various distances from the duct wall and inlet. The Reynolds number based on the hydraulic diameter and the bulk velocity was varied between 7.5×10^3 and 18.6×10^3. An empirical equation for the entrance length required for fully developed turbulent flow was obtained and this was compared with experimental results.

Turbulent flow in a duct: Measurement by a tracer gas technique

S B Riffat Dipl Tech MSc DPhil MASHRAE CEng MIMechE MInstE and **S F Lee** Dipl Tech
Department of Civil Engineering, Loughborough University of Technology, Loughborough, Leicestershire, LE11 3TU, UK

Received 27 April 1989, in final form 21 August 1989

List of symbols

V	Internal volume of the duct (m^3)
C	Concentration of tracer gas (ppm)
C_0	Concentration of tracer gas at $t = 0$ (ppm)
$\dot{C}$	Rate of change of concentration of tracer gas (ppm s^{-1})
C_b	Average concentration of tracer gas at the duct inlet (ppm)
C_m	Centre line concentration in the fully developed region of the duct (ppm)
F	Volumetric flow rate ($m^3 s^{-1}$)
q	Injection flow rate of tracer gas ($m^3 s^{-1}$)
I	Air exchange rate (h^{-1})
P	Pressure (Pa)
h_a	Pressure at point a (Figure 2) (mm H_2O)
h_x	Static pressure at point x along the duct (mm H_2O)
U	Local time mean velocity (m s^{-1})
U_b	Bulk velocity (m s^{-1})
U_m	Maximum velocity in the fully developed region (m s^{-1})
U_c	Centre line velocity (m s^{-1})
U_τ	Friction velocity (m s^{-1})
g	Acceleration due to gravity (m s^{-2})
ρ	Air density (kg m^{-3})
ρ_w	Water density (kg m^{-3})
A_A	Internal cross-sectional area of the bellmouth at section A (Figure 2) (m^2)
A_B	Internal cross-sectional area of the duct at section B (Figure 2) (m^2)
f	Friction factor
Z	Intercept of static pressure lines (mm H_2O)
τ_w	Wall shear stress (Pa)
Re	Reynolds number
L_e	Entrance length for fully developed flow (m)
D_h	Hydraulic diameter of the duct (m)
X	Distance from the duct inlet in the direction of flow (m)
y	Distance from the wall of the duct (mm)
t	Time (s)
H	Duct height (m)
W	Duct width (m)
L	Length to pressure taps (which have been used to determine (dP/dx))

1 Introduction

The analysis of turbulent flow through ducts has considerable engineering importance in the design of fluid transporting systems such as HVAC systems, atomic power reactors, gas turbines and heat exchangers. Turbulent flow in ducts of various roughnesses, lengths and aspect ratios has been investigated previously using hot-wire anemometers, laser doppler velocimeters and pitot tubes[1–3]. The use of tracer gas techniques offers an alternative approach to work reported to date and offers the opportunity to develop improved air flow formulae. Tracer gas techniques have been widely used for measuring air flow in buildings[4–6] but only limited work has been published on the use of tracer gas techniques for the measurement of air flow in ducts[7–8]. There is a need to carry out a detailed study to determine the applicability of these techniques to the investigation of turbulent flow in ducts.

This paper describes the use of the constant injection tracer gas method for the estimation of air flow in a smooth duct. We have implemented this tracer gas technique to determine the entrance length L_e required for fully developed turbulent flow. Results derived from tracer gas measurements are compared with data obtained using a hot-wire anemometer and a pitot tube.

2 Fundamentals of the constant-injection tracer-gas technique

The constant-injection tracer-gas technique can be used to measure air flow in ducts. Assuming that the air and tracer gas are perfectly mixed within the duct and that the concentration of the tracer gas in the outside air is zero, the mass balance equation is:

$$V\dot{C}(t) + F(t)C(t) = q(t) \tag{1}$$

The duct air exchange rate I is given by:

$$I(t) = F(t)/V \tag{2}$$

Assuming that the injection rate of tracer gas into the duct and the duct air exchange rate are constant during the measurement, the solution of equation (1) is:

$$C(t) = q/F + (C_0 - q/F)\exp(-It) \tag{3}$$

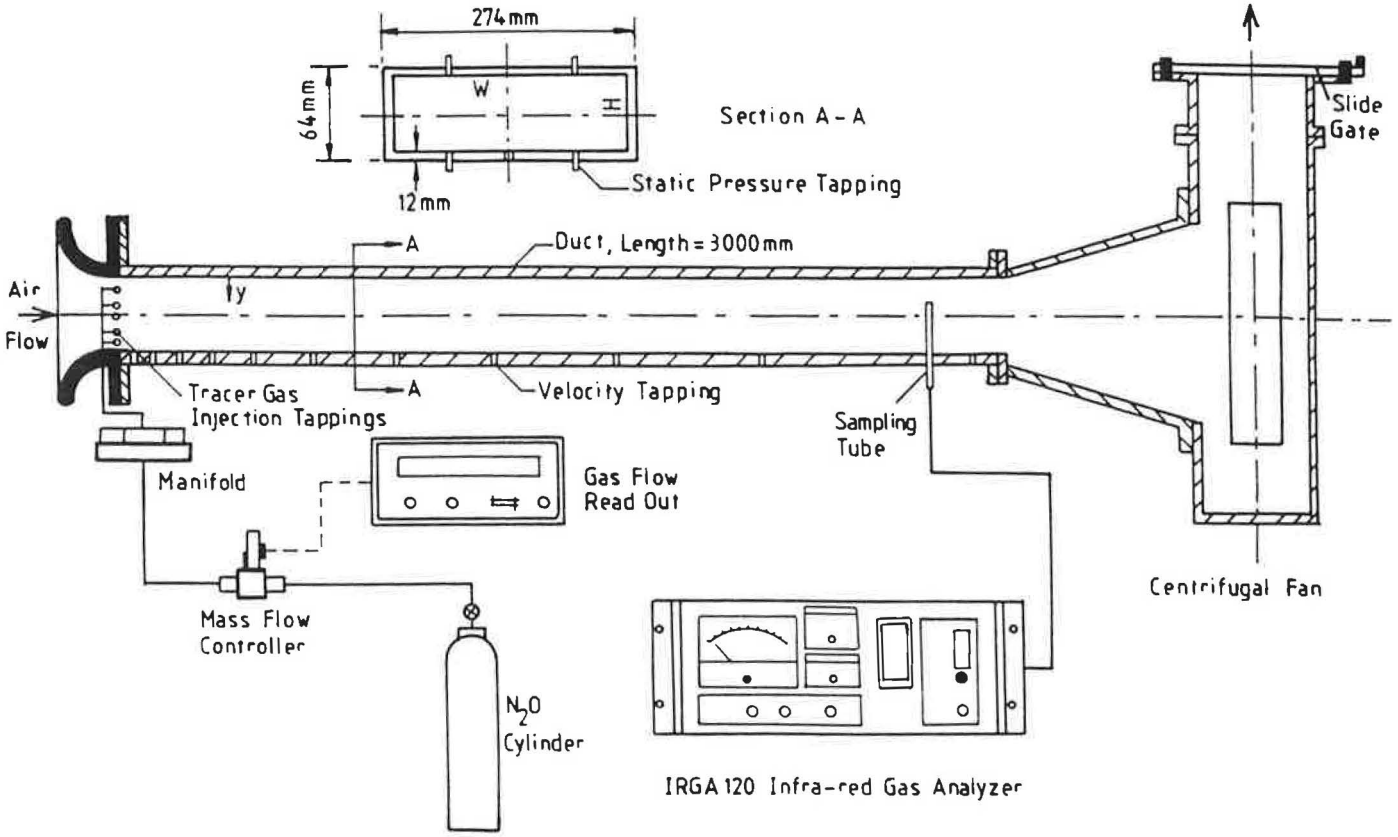

Figure 1 Schematic diagram of the experimental system

If the system were close to equilibrium, the concentration of tracer gas would change slowly and the rate of change of concentration of tracer gas would be small. After a sufficiently long period, the transient term in equation 3 would die out and the flow rate through the duct would simply be given by:

$$C = q/F \tag{4}$$

Hence, if measurements of tracer gas flow rate and concentration can be made, F can be evaluated.

3 Experimental apparatus and instrumentation

The duct shown in Figure 1 was constructed from 12 mm thick plywood. The entrance to the duct consisted of a bellmouth made from wooden bars. The duct was 3 m long and had an internal cross-section of 250 × 40 mm (i.e. the aspect ratio W/H of the duct was 6.25). The downstream end of the duct was connected to the suction side of a centrifugal fan by means of a diffuser. The flow rate of air through the duct was varied using a slide gate located at the discharge end of the fan. The centrifugal fan was driven by a 335 W AC motor.

Static and velocity pressure tappings were distributed at various positions ($X/D_h = 4.1$ to 134) along the duct as shown in Figure 1. The velocity tappings allowed the insertion of a pitot tube or a hot wire anemometer. These could be traversed across the duct cross-section in order to measure velocity at various distances from the wall. A single tube inclined manometer, made by Air Flow Development Ltd, UK, was used to measure the static and velocity pressure heads.

The nitrous oxide tracer gas was injected at a constant rate into the duct inlet via a number of small injection tappings distributed around the perimeter of the duct. These tappings were connected to a manifold using flexible tubing. Nitrous oxide gas was supplied to the manifold via a type F-100/200, mass flow controller which had maximum capability of 1 l min^{-1} and was manufactured by Bronkhorst High-Tech B V, Holland. The measurement accuracy of the mass flow controller was ±1%. The flow rate was controlled using a variable power supply and the rate of tracer gas injection was displayed on a digital unit.

Tracer gas/air samples were collected using a sampling tube which could be positioned at various points along the length of the duct. This tube was mounted on a traversing mechanism which allowed samples to be taken at various distances from the duct wall. The air flow rate through the duct was estimated, using equation 4, by measuring the concentration of tracer gas in the air upstream from the fan.

The concentration of N_2O tracer gas was measured using an IRGA 120 Infra-red Gas Analyser. The instrument, manufactured by J and S Sieger Ltd, UK, was a two-beam gas analyser equipped with a gas filled detector of the Luft type. The two beams of infra-red radiation of equal energy were interrupted at 6.6 Hz by a rotating shutter. These two series of pulses of infra-red energy passed simultaneously, one through an analysis cell, the other through a parallel reference cell, into a detector. The detector consisted of two sealed absorption chambers separated by a thin diaphragm. The absorption chambers were filled with a quantity of gas (N_2O) for which the instrument was calibrated. The amount of infra-red absorption was measured and converted to parts per million (ppm) for a direct readout on a meter.

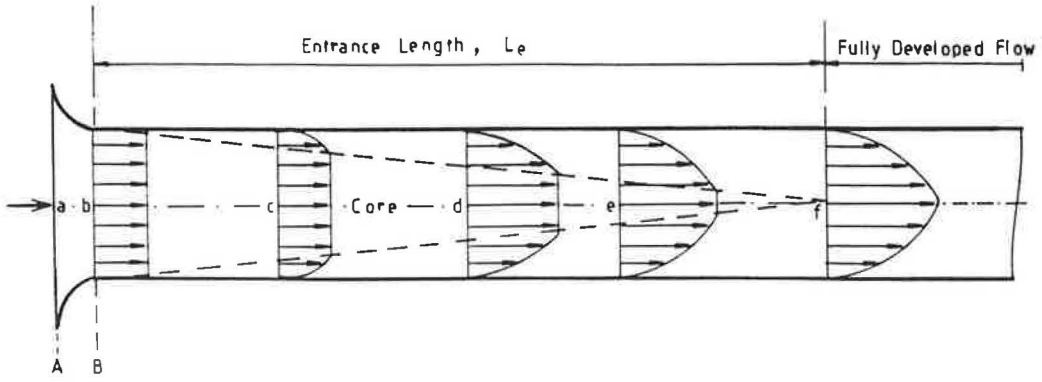

Figure 2 Development of turbulent flow in a two-dimensional duct

4 Analysis of turbulent flow in a duct

The formation of a boundary layer in a duct is shown in Figure 2. Air enters the duct at point a with a velocity U_a. At point b the velocity is uniform across the section of the duct. At point f the boundary layer is completely formed. Further downstream from point f the boundary layer has a constant thickness. Here the influence of the entrance shape upon the air flow pattern has disappeared and fully developed flow is said to exist.

We carried out measurements of tracer gas concentration and pressure distribution along the duct for a range of Reynolds numbers. Figures 3, 4 and 5 were used to develop an expression for the entrance length required for turbulent flow to be fully developed (equation 5). The full derivation is given in the Appendix.

$$L_e/D_h = (0.2 + 2.265 \times 10^{-4}\,\mathrm{Re})\,\mathrm{Re}^{0.25} \qquad (5)$$

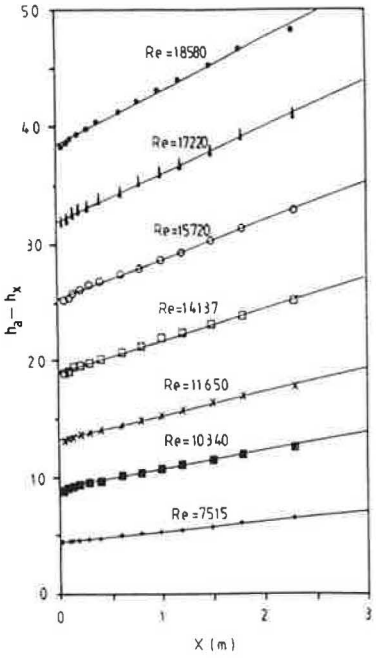

Figure 4 Static pressure distribution along the duct for various values of Re

5 Results and discussion

The tracer gas constant injection method, a hot-wire anemometer and a pitot tube were used to measure turbulent air flow in the fully developed region of the duct (i.e. $X/D_h = 105$). Figure 6 shows a comparison between measurements of duct air flow rates made using the tracer gas technique and measurements made using a hot-wire anemometer and a pitot tube. The tracer gas results were generally found to be in good agreement with those obtained using the hot-wire and the pitot tube. However, there were uncertainties in

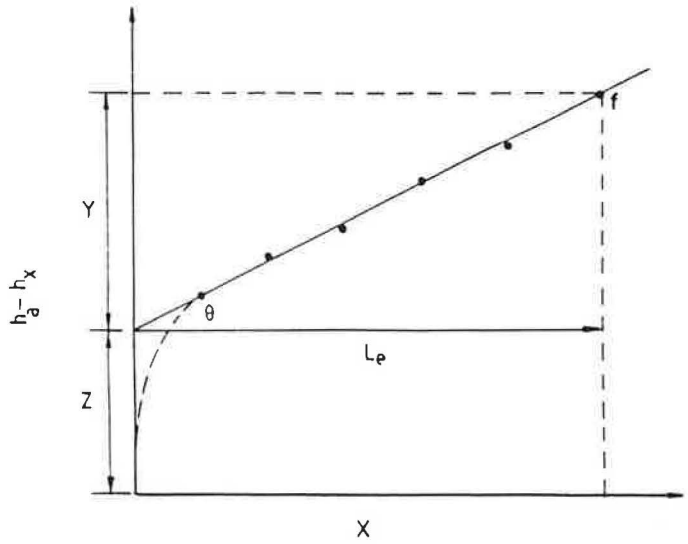

Figure 3 Variation of static pressure with X

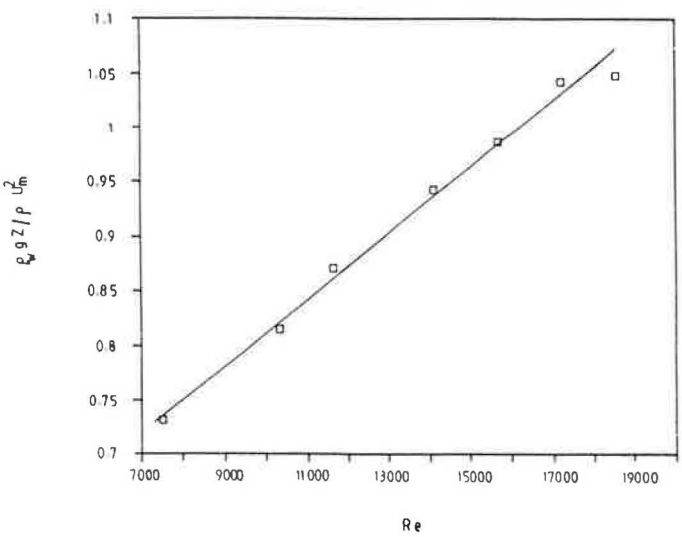

Figure 5 Variation of $\rho_w gZ/\rho U_m^2$ with Re

the measurements as both the hot-wire and pitot tube are sensitive to alignment with the flow as well as to turbulence level. The difficulty in measuring the velocity close to the duct wall and the internal cross-sectional area of the duct causes additional errors.

We also carried out measurement of centre line velocity along the length of the duct for various Reynolds numbers. The velocity was determined using the constant injection technique as well as the hot-wire anemometer and pitot tube. The concentration of tracer gas was measured at different distances from the duct wall and from the duct inlet. The maximum flow rate was calculated using equation 4 and the measured centre line concentration. The centre line velocity was then calculated by dividing the maximum flow rate by the cross sectional area of the duct. As the hot-wire anemometer and pitot tube measurements were strongly influenced by the disturbances caused by the entrance configuration of the duct, all measurements were carried out at X/D_h greater than 21.9. Figure 7 shows a typical variation of centre line velocity for different values of X/D_h. The tracer gas was injected at a position $X/D_h = 21.9$ and the concentration in air was monitored at various positions downstream. Due to poor mixing of tracer gas close to the injection point, the estimated velocities were found to be less than those measured using the hot-wire and pitot tube. However, for fully developed flow the results were in closer agreement and the estimated velocities from the tracer gas measurements lay between those obtained using the hot-wire and the pitot tube.

The variation of tracer gas concentration along the length of the duct for various Reynolds numbers is shown in Figure 8. The concentration of tracer gas was found to decrease at the inlet of the duct as X/D_h increased. The concentration of tracer gas remained constant when the flow was fully developed. For low Re a large X/D_h was required for the concentration of tracer gas to reach a constant value.

Measurement of velocity (using a pitot tube) at various distances from the duct wall was also carried out. Turbulent velocity profiles for $Re = 1.4 \times 10^4$ and different values of X/D_h are presented in Figure 9. It is apparent that the velocity profile changes shape from one section to another

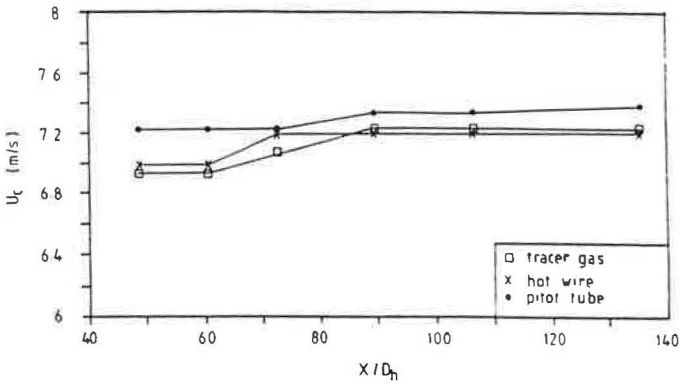

Figure 7 Variation of centre-line velocity with X/D_h

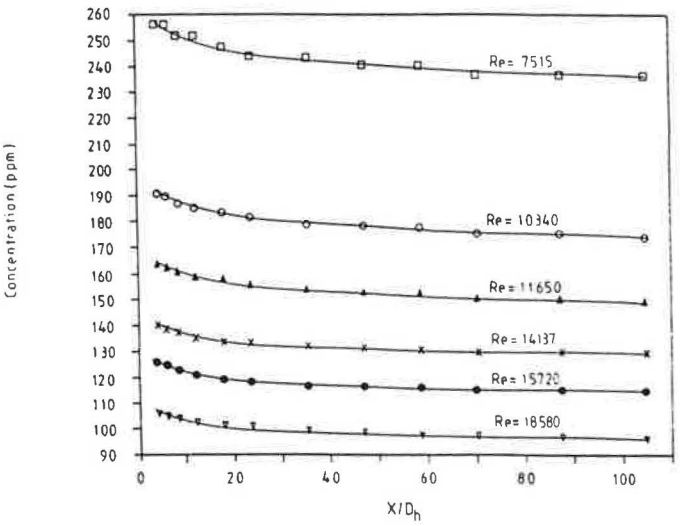

Figure 8 Variation of tracer gas concentration with X/D_h for various values of Re

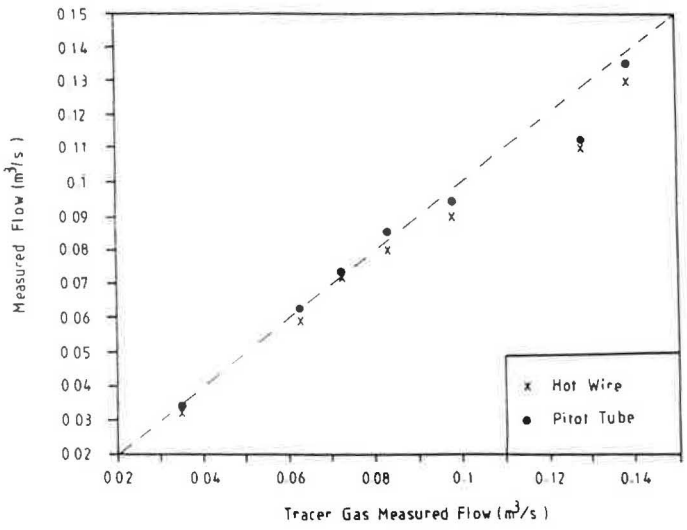

Figure 6 Comparison of tracer gas duct air flow measurements with measurements made using a hot-wire anemometer and a pitot tube

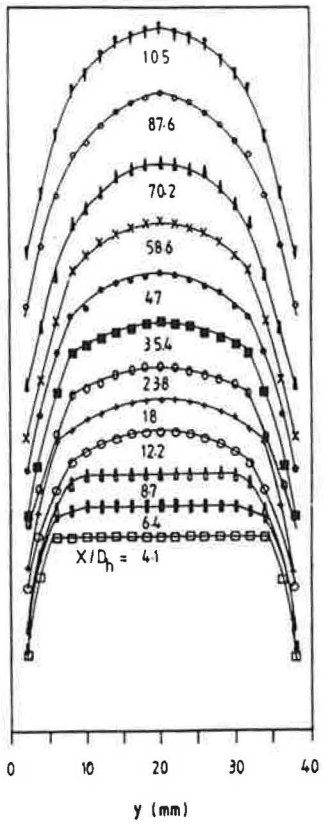

Figure 9 Turbulent velocity profiles at various distances from the duct entrance

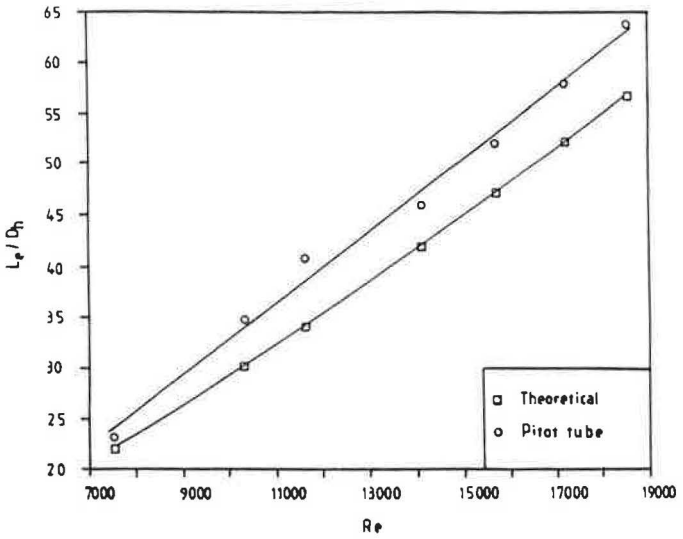

Figure 10 Variation of L_e/D_h with Re

in accordance with boundary layer development. For other Reynolds numbers, velocity profiles along the duct were found to behave in a similar manner.

The analysis to determine the entrance length required for fully developed flow shows that:

$$L_e/D_h = (0.2 + 2.265 \times 10^{-4}\,\mathrm{Re})\,\mathrm{Re}^{0.25} \quad (5)$$

From the pitot tube measurements of velocity distribution at various X/D_h, the following equation is obtained:

$$L_e/D_h = -2.276 + 0.00352\,\mathrm{Re} \quad (6)$$

The variation of L_e/D_h versus Re is shown in Figure 10. For turbulent flow with Re greater than 16 000, an entrance length greater than 50 hydraulic diameter was necessary for the formation of a fully developed velocity profile. The entrance length predicted by the empirical equation was found to be 0.1 to 0.2 m less than that obtained from the pitot tube measurements. Equations 5 and 6 are only applicable to ducts of a similar type to the one used in our work as the formation of fully developed flow depends on factors such as the entrance configuration, the turbulence of the entering stream, the aspect ratio and the roughness of the duct.

6 Conclusions

The use of the constant injection tracer gas technique was found to be a convenient means for measuring air flow in ducts. Estimated air flow derived from measurements made using the tracer gas technique was found to be in good agreement with that obtained from measurements made using a hot wire anemometer and a pitot tube.

Tracer gas measurements were used to derive an equation describing the entrance length for fully developed flow in the duct configuration under test. The empirical equation predicted an entrance length 0.1 to 0.2 m less than that obtained from pitot tube measurements.

Appendix

Considering Figure 2, and applying the continuity equation to sections A and B, we have:

$$A_A U_A = A_B U_B \quad (A1)$$

But $U_A = U_a$ and $U_B = U_b$ and so equation A1 can be rewritten as

$$U_a = U_b A_B / A_A \quad (A2)$$

Applying Bernoulli's equation between points a and f (along the stream line abf, Figure 2) gives:

$$U_a^2/2g + P_a/\rho g = U_f^2/2g + P_f/\rho g \quad (A3)$$

But $U_f = U_m$

Substituting equation 2 into equation 3 and rearranging, we have:

$$(P_a - P_f)/\rho g = [U_m^2 - (A_B/A_A)^2 U_b^2]/2g \quad (A4)$$

Dividing both sides of equation A4 by U_m^2 we have:

$$(P_a - P_f)/\rho U_m^2 = 0.5 - 0.5(A_B/A_A)^2(U_b/U_m)^2 \quad (A5)$$

But $A_B/A_A = 0.183$

Tracer gas concentration was measured at different distances from the duct wall at the inlet of the duct and at the region of fully developed flow. This allowed the ratio C_m/C_b to be determined. Applying equation 4, we find that the flow rate ratio is given by:

$$F_b/F_m = C_m/C_b$$

since

$$F = AU$$

the velocity ratio U_b/U_m is given by:

$$U_b/U_m = F_b/F_m = C_m/C_b$$

The average value of U_b/U_m for the range of Reynolds numbers used in these experiments was 0.916.

Substituting the values of A_B/A_A and U_b/U_m into equation A5 gives:

$$(P_a - P_f)/\rho U_m^2 = 0.486 \quad (A6)$$

Consider the variation of static pressure with X, Figure 3. The difference between the static pressure at $X = 0$ (i.e. pressure $\approx$ atmospheric pressure) and the static pressure of fully developed flow, $X = L_e$ is given by:

$$h_a - h_x = (Z + Y) = Z + L_e \tan\theta \quad (A7)$$

or

$$h_a - h_x = Z + L_e\,\mathrm{d}h_x/\mathrm{d}x \quad (A8)$$

For fully developed flow, $h_x = h_f$. Multiplying both sides of equation A8 by $\rho_w g$ we have:

$$P_a - P_f = \rho_w g Z + L_e \mathrm{d}P/\mathrm{d}x \quad (A9)$$

From Reference 9

$$\tau_w = -(D_h/4)\mathrm{d}P/\mathrm{d}x \quad (A10)$$

Equation A10 is normally applied to regions of fully developed flow but is also a very good approximation[9,10] for the entrance region of the duct provided that $L/D_h \gg 1$. Experimental results (Figure 4) showed that $\mathrm{d}P/\mathrm{d}x$ was constant along the length of the duct for the range of Reynolds numbers used.

Substituting equation A10 into A9 and dividing both side of equation A9 by ρU_m^2, we have:

$$(P_a - P_f)/\rho U_m^2 = \rho_w g Z/\rho U_m^2 - 4 L_e \tau_w / D_h \rho U_m^2 \quad (A11)$$

From Reference 9

$$U_\tau = (\tau_w/\rho)^{0.5} \quad \text{(A12)}$$

and

$$U_\tau = U_b(f/2)^{0.5} \quad \text{(A13)}$$

Substituting equations A12 and A13 into equation A11 and simplifying, we have:

$$(P_a - P_f)/\rho U_m^2 = \rho_w g Z/\rho U_m^2 - 2(L_e f/D_h)(U_b/U_m)^2 \quad \text{(A14)}$$

From tracer gas measurements, $U_b/U_m = 0.916$

and from Reference 9

$$f = 0.079\,\mathrm{Re}^{-0.25} \quad \text{(A15)}$$

Equation A15 is applicable when the velocity profile is fully developed. If the velocity profile is not fully developed but $L/D_h \gg 1$, then equation 15 is a good approximation[9,10].

Substituting the value of U_b/U_m and equation A15 into A14 and simplifying, we have

$$(P_a - P_f)/\rho U_m^2 = \rho_w g Z/\rho U_m^2 - 0.1325\,(L_e/D_h)\mathrm{Re}^{-0.25} \quad \text{(A16)}$$

Substituting equation A6 into A16 and simplifying, we have:

$$L_e/D_h = 7.55\rho_w g Z/\rho U_m^2 - 3.66\,\mathrm{Re}^{0.25} \quad \text{(A17)}$$

The intercepts Z of the static pressure lines were found from Figure 4. Figure 5 shows a plot of $\rho_w g Z/\rho U_m^2$ versus Re. The best fit was used to determine the following equation:

$$\rho_w g Z/\rho U_m^2 = 0.5112 + 0.00003\,\mathrm{Re} \quad \text{(A18)}$$

Substituting equation A18 into equation A17 we obtain:

$$L_e/D_h = (0.2 + 2.265 \times 10^{-4}\,\mathrm{Re})\mathrm{Re}^{0.25} \quad \text{(A19)}$$

This equation can be used to determine the entrance length L_e for fully developed turbulent flow.

References

1 Hussain A K M F and Reynolds W C Measurements in fully developed turbulent channel flow *J. Fluid Eng. Trans. ASME* **97** 568–580 (1975)

2 Liou T and Lin J Measurement of turbulent flow in a duct with repeated ribs applied to opposite walls *J. Chinese Inst. Engineers* **11**(4) 319–326 (1988)

3 Hartnett J P, Koh J C Y and McComas S T A comparison of predicted and measured friction factors for turbulent flow through rectangular ducts *J. Heat and Mass Transfer, Trans. ASME* 82–88 (1962)

4 Riffat S B and Eid M Measurement of air flow between the floors of houses using a portable SF_6 system *Energy and Building* **12**(1) 67–75 (1988)

5 Riffat S B Interzone air movement and its effect on condensation in houses *Applied Energy* **32**(1) 49–69 (1989)

6 Lagus L and Persily A K A review of tracer-gas techniques for measuring airflows in buildings *ASHRAE Trans.* **91**(2B) (1) 1075–1087 (1985)

7 Lundin L Air leakage in industrial buildings-preliminary results *Proc. 4th AIVC Conference Air Infiltration Reduction in Existing Buildings (Elm, Switzerland)* pp 6.1–6.8 (September 1983)

8 Axley J and Persily A Integral mass balances and pulse injection tracer gas techniques *Proc. 9th AIVC Conf. Effective Ventilation, Gent, Belgium*, paper no. 7 (September 1987)

9 Brid R B, Stewart W E and Lightfoot E N *Transport Phenomena* (New York: Wiley) (1960)

10 Dean R B Reynolds number dependence of skin friction and other bulk flow variables in two-dimensional rectangular duct flow *J. Fluid Engineering* **100** 215–222 (1978)